PROCEEDINGS OF SCIENCE

On the quarks transverse momenta in SIDIS experiments

Michail Stoilov[a,*]

[a] *Institute for Nuclear Researches and Nuclear Energy*
Bulgarian Academy of Sciences,
Tzarigradsko Chaussee 72, Sofia, Bulgaria

E-mail: mstoilov@inrne.bas.bg

In a series of recent papers we have suggested to use the information on the so-called Difference Asymmetries in Semi-Inclusive Deep Inelastic Scattering in order to determine the Boer-Mulders function for the sum of valence quarks. We have also determined the kinematical Cahn contribution, both directly from a fit to the data (as far as we know for the first time) and from a calculation. Here we comment on how our analysis can be used to find the parameters of the quarks and hadrons transverse momenta distributions.

11th International Conference of the Balkan Physical Union (BPU11),
28 August - 1 September 2022
Belgrade, Serbia

*Speaker

PoS(BPU11)100

1. Introduction

The Feynman parton model [1] gives a good description of the hadrons high energy reactions on the base of simple QCD calculations and few phenomenologically determined functions — parton distribution functions (PDFs) and fragmentation functions (FFs). The recent data shows however that the initial simple picture of collineary moving partons has to be substituted with more complicated one where partons have transverse momenta. In this new picture different new PDFs and FFs are needed which have to be determine from the experiment.

In the present research we are focused on one of these new functions, namely the Boer-Mulders (BM) one, using the data on semi-inclusive deep inelastic scattering (SIDIS) of leptons on nucleons. The BM function [2] describes the distribution inside an unpolarized nucleon of transversely polarized quarks. It is a leading twist, chiral odd, transverse momentum dependent parton distribution. The main problem is that there is no sufficient data for its direct determination and therefore some assumptions have to be made. In the first attempts to extract BM function (from data on Drell-Yan reactions) its proportionality to the better known Sivers function [3] for *each* quark flavor has been assumed, assumptions motivated by model calculations [4–6]. However, as it is explained in Ref.[7], these assumptions are theoretically inconsistent because they lead to gluons contribution in the Q^2 evolution of non-singlet combinations of quark densities. In the same paper we show that the new COMPASS data on the $\langle \cos \phi_h \rangle$ and $\langle \cos 2\phi_h \rangle$ asymmetries in SIDIS reactions on deuteron target with production of hadron h and its anti particle $\bar{h}$ at azimuthal angle ϕ_h allows the extraction of the BM function of valence quarks with only *one* model dependent assumption. In our analysis we use the so-called difference asymmetries [8, 9], i.e. the difference between the asymmetries in the production of particles and their anti particles from polarized and unpolarized target. In this way we successfully carry out two independent consistency tests of our single assumption of proportionality. Here we try to use the results of the analysis in order to determine the parameters of transverse momentum distributions in BM and Collins functions.

The paper is organized as follows: First, we give some basic facts about SIDIS and the used notations and functions to describe it. We also enlist the implicit assumptions made in the SIDIS considerations. Second, we outline the test of our basic assumption using COMPASS data and prove its validity. Third, on the base of the results of the tests we make some comments on the quarks transverse momenta in SIDIS experiments.

2. Semi-Inclusive Deep Inelastic Scattering

In the SIDIS processes [10] a lepton l scatters from a target nucleon N. After the collision one detects the scattered lepton l', and a hadron h generated from the fragmentation of a scattered in azimuthal direction ϕ_h quark. The final lepton and hadron momenta are detected as well. There are two variant of SIDIS processes — with unpolarized and with polarized target

$$l + N \rightarrow l' + h + X \tag{1}$$

$$l + N^{\uparrow} \rightarrow l' + h + X, \tag{2}$$

where X denotes the other particles, produced in the process, which remain undetected. The notation $N^{\uparrow}$ in eq.(2) means that the target is polarized, so the azimuthal angle ϕ_S of the target

nucleon spin with respect to $l - l'$ plane is known. The kinematics of the process in the center of mass coordinate system is illustrated on Fig. 1.

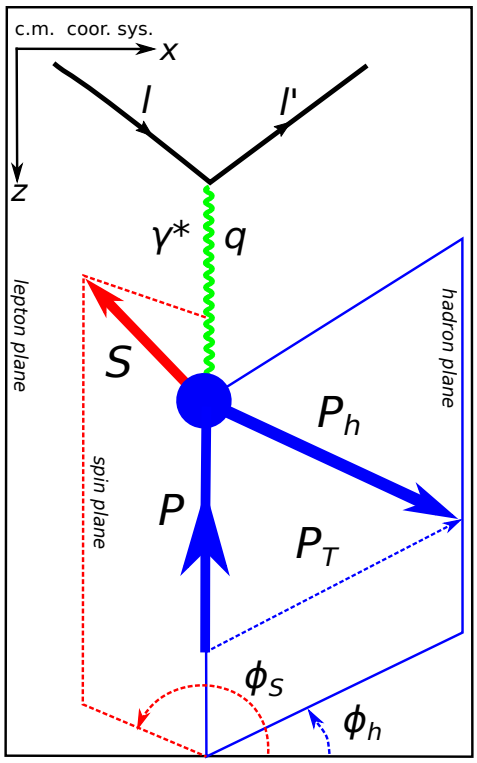

Figure 1: SIDIS kinematics. See the text for notations.

SIDIS experiments allow to collect some new information on partons encoded in the so-called Transverse Momentum Dependent Partonic Distribution and Fragmentation Functions (TMD-PDFs and TMD-FFs, or, shortly, TMDs), $\hat{f}_{a\,N}(x_B, k_\perp)$ (which give the number density of quarks (a = q) or gluons (a = g) with light-cone momentum fraction x_B and transverse momentum $k_\perp$ inside a fast moving nucleon N and $\hat{D}_{h\,a}(z_h, p_\perp)$ (which give the number density of hadrons h resulting in the fragmentation of parton a, with a light-cone momentum fraction z_h and a transverse momentum $p_\perp$, relative to the original parton motion). The SIDIS cross section is factorizable, i.e.

$$d\sigma^{l\,N\to l'\,h\,X} = \sum_q \hat{f}_{q\,N}(x_B, k_\perp; Q^2) d\sigma^{lq\to l'q} \hat{D}_{h\,q}(z_h, p_\perp; Q^2), \tag{3}$$

where the sum is over all quarks q and $d\sigma^{lq\to l'q}$ are the quark – lepton cross sections given by QCD.

The cross section (double) Fourier Series Expansion over the angles ϕ_h and $\phi_S - \phi_h$ is used in

the analysis [10]:

$$\begin{aligned}\frac{d\sigma^h}{dx_B\, dQ^2\, dz_h\, d^2\mathbf{P}_T d\phi_S d\phi_h} &= \frac{2\pi\alpha_{em}^2}{Q^4}\Big\{[1+(1-y)^2]\, F_{UU}^{0,0,h} + \\ &+2(2-y)\sqrt{1-y}\,\cos\phi_h\, F_{UU}^{1,0,h} + \\ &+2(1-y)\,\cos 2\phi_h\, F_{UU}^{2,0,h} + \\ &+ S_T(1+(1-y)^2)\,\sin(\phi_S-\phi_h)\, F_{UT}^{0,1,h} + \ldots\Big\}. \end{aligned} \tag{4}$$

Here $F^{n,m,h}$ are the Fourier components corresponding to $\cos(n\phi_h)\times\sin(m(\phi_S-\phi_h))$ terms in the double Fourier Series Expansion with the proper y-dependence explicitly factorized. All $F^{n,m,h}$ are functions of x_B, Q^2, z_h and $\mathbf{P}_T$. Note that only terms relevant to our investigation are written down in eq.(4). Other notations used in fig.1 and eq.(4): l and P are the initial lepton and nucleon 4-momenta, l' and P_h are the final lepton and (final) hadron 4-momenta, $z_h = (P\cdot P_h)/(P\cdot q)$, where $q = l - l'$ is the transferred momentum (the momentum of virtual photon γ^*), $y = (P\cdot q)/(P\cdot l)$, $Q^2 = -q^2 = 2M_N E x_B y$ (which is in the same time a definition of Bjorken parameter x_B) where M_N is the target mass (in our case this is the deuteron mass M_d), E is the lepton laboratory energy, S_T is the nucleon polarization, P_T is the (measured) transverse momentum of the final hadron, which (at order $k_\perp/Q$) is $P_T = z_h k_\perp + p_\perp$.

The most economic way to retrieves TMDs from experiments is to use the so called difference asymmetry:

$$A^{h-\bar{h}} \equiv \frac{\Delta\sigma^h - \Delta\sigma^{\bar{h}}}{\sigma^h - \sigma^{\bar{h}}}. \tag{5}$$

Here, $\bar{h}$ stands for the anti particle of hadron h. The quantities with Δ prefix refer to polarized target and those without Δ — to unpolarized target. The basic advantages of the approach using difference asymmetries [9] are that first, the results are expressed only in terms of the valence-quark distributions and fragmentation functions and second, for a deuteron target, independently of the final hadron, only the sum of the valence-quark distributions enters.

Eq.(5) can be recast in the following form:

$$A^{h-\bar{h}} = \frac{1}{1-r}\left(A^h - r\, A^{\bar{h}}\right) \tag{6}$$

where

$$A^h = \frac{\Delta\sigma^h}{\sigma^h},\quad A^{\bar{h}} = \frac{\Delta\sigma^{\bar{h}}}{\sigma^{\bar{h}}},\quad r = \frac{\sigma^{\bar{h}}}{\sigma^h}. \tag{7}$$

The corresponding x_B-dependent asymmetries, integrated over P_T^2, z_h and Q^2, that we shall work with, in terms of the quantities defined in eq.(4) are:

$$A_{UU}^{\cos\phi_h, h-\bar{h}}(x_B) = \frac{\int dQ^2\, dz_h\, dP_T^2\, [(2-y)\sqrt{1-y}/Q^4]\,(F_{UU}^{1,0,h} - F_{UU}^{1,0,\bar{h}})}{\int dQ^2\, dz_h\, dP_T^2\, [[1+(1-y)^2]/Q^4]\,(F_{UU}^{0,0,h} - F_{UU}^{0,0,\bar{h}})} \tag{8}$$

$$A_{UU}^{\cos 2\phi_h, h-\bar{h}}(x_B) = \frac{\int dQ^2\, dz_h\, dP_T^2\, [(1-y)/Q^4]\,(F_{UU}^{2,0,h} - F_{UU}^{2,0,\bar{h}})}{\int dQ^2\, dz_h\, dP_T^2\, [[1+(1-y)^2]/Q^4]\,(F_{UU}^{0,0,h} - F_{UU}^{0,0,\bar{h}})} \tag{9}$$

$$A_{UT}^{Siv, h-\bar{h}}(x_B) = \frac{1}{S_T}\frac{\int dQ^2\, dz_h\, dP_T^2\, [[1+(1-y)^2]/Q^4]\,(F_{UT}^{0,1,h} - F_{UT}^{0,1,\bar{h}})}{\int dQ^2\, dz_h\, dP_T^2\, [[1+(1-y)^2]/Q^4]\,(F_{UU}^{0,0,h} - F_{UU}^{0,0,\bar{h}})}. \tag{10}$$

From the phenomenological point of view (see eq.(3)) several collinear PDFs and FFs and non-collinear TMDs are used in the description of eqs.(8–10). Here we focus ourselves on Sivers and Boer–Mulders PDFs and Collins FFs. The Sivers function $\Delta f^{Q_V}_{Sivers}(x_B, k_\perp, Q^2)$ describes the correlation between the spin of the nucleon $\mathbf{S}$, its momentum $\mathbf{P}$, and the transverse momentum of the quark $\mathbf{k}_\perp$, via a term proportional to $\mathbf{S}\cdot(\mathbf{k}_\perp\times\mathbf{P})$ [3]. The BM function $\Delta f^{Q_V}_{BM}(x_B, k_\perp, Q^2)$ describes the correlation between the spin of the quark $\mathbf{s}_q$ and the momentum of the quark $\mathbf{k}_\perp$, via a term proportional to $\mathbf{s_q}\cdot(\mathbf{k}_\perp\times\mathbf{P})$ [2]. The Collins FFs $\Delta^N D_{h/q\uparrow}(z, p_\perp)$ describe phenomenologically the spin-dependent part of the fragmentation functions of transversely polarized quarks, with transverse spin $\mathbf{s}_q$ and 3-momentum $\mathbf{p}_q$, into hadrons h with momentum $\mathbf{p}_\perp$, transverse to the direction of the initial quark [15] $D_{h/q,s}(z_h, p_\perp) = D_{h/q}(z_h, p_\perp) + \frac{1}{2}\Delta^N D_{h/q\uparrow}(z_h, p_\perp)\,\hat{\mathbf{s}}_q\cdot(\hat{\mathbf{p}}_q\times\hat{\mathbf{p}}_\perp)$ thus leading to nonuniform azimuthal distribution of final hadrons around the initial quark direction.

Hereafter we shall work with PDFs and FFs which satisfy several assumptions. First, we choose to work with data in the Q^2 interval where the Q^2-dependence of the collinear PDF's and FFs can be neglected. In the COMPASS kinematics to each value of $\langle Q^2\rangle$ corresponds one definite value of $\langle x_B\rangle$, thus fixing the Q^2 interval we fix the x_B interval as well. Second, we assume some relations between collinear and non-collinear PDFs and FFs (see below for details). Third, we assume some factorization of PDFs and FFs. Forth, we assume very simple dependence on transverse momenta where only parameter is needed. More specifically:

$$\Delta f^{Q_V}_J(x_B, k_\perp, Q^2) = \underbrace{\Delta f^{Q_V}_J(x_B, Q^2)}_{2\,\mathcal{N}^{Q_V}_J(x_B)\,Q_V(x_B, Q^2)} \sqrt{2e}\,\frac{k_\perp}{M_J}\,\frac{e^{-k_\perp^2/\langle k_\perp^2\rangle_J}}{\pi\,\underbrace{\langle k_\perp^2\rangle_J}_{\frac{\langle k_\perp^2\rangle M_J^2}{\langle k_\perp^2\rangle + M_J^2}}}. \tag{11}$$

Here: $J = BM,\ Sivers$; Q_V stands for $u_V + d_V$; $\mathcal{N}^{Q_V}_J(x_B)$ are unknown functions, $Q_V(x_B, Q^2) = u_V(x_B, Q^2) + d_V(x_B, Q^2)$, where $u_V(x_B, Q^2)$ and $d_V(x_B, Q^2)$ are the corresponding valence quarks collinear PDFs (the valence quark distribution q_V is the difference between corresponding quark and anti quark distributions); M_J, or equivalently $\langle k_\perp^2\rangle_J$, are unknown parameters. Note that the Normal distribution on $k_\perp$ is an assumption too which can be tested.

Having in mind the very close definitions of Boer–Mulders and Sivers function we make the following assumption:

$$\Delta f^{Q_V}_{BM}(x, k_\perp, Q^2) = \lambda_{Q_V}\,\Delta f^{Q_V}_{Siv}(x, k_\perp, Q^2), \tag{12}$$

where λ_{Q_V} is some constant. Note that, as it has been mentioned earlier, the differential asymmetries depends only on the sum of valence quark distributions. This fact extremely simplifies the used formulas, but also limits the hypotheses we can check. Thus, assuming proportionality between BM and Sivers functions, eq.(12) is the only one, we can test using differential asymmetries extracted from deuteron data. The much stronger assumption that Boer–Mulders and Sivers function are proportional for each and every quark separately has been considered in Refs.[11, 12]. Obviously, it can not be checked in the way considered here. We shall comment on the relation between both assumption a bit later.

From eq.(12) we have:

$$\begin{aligned} M_{BM} &= M_S, \\ \langle k_\perp^2 \rangle_{BM} &= \langle k_\perp^2 \rangle_S \\ \mathcal{N}_{BM}^{Q_V}(x_B) &= \lambda_{Q_V}\, \mathcal{N}_{Siv}^{Q_V}(x_B). \end{aligned} \tag{13}$$

In terms of difference asymmetries we have:

$$A_{UT,d}^{Siv,h-\bar{h}}(x_B) = \frac{\sqrt{e\pi}}{2\sqrt{2}}\, A_{Siv}\, \underbrace{C_{Siv}^h}_{\text{const.}}\, \mathcal{N}_{Siv}^{Q_V}(x_B), \tag{14}$$

where $A_{Siv} = \frac{\langle k_\perp^2 \rangle_S^2}{M_S \langle k_\perp^2 \rangle}$. Therefore:

$$\mathcal{N}_{BM}^{Q_V}(x_B) = \lambda_{Q_V}\, \frac{2\sqrt{2}}{\sqrt{e\pi}}\, \frac{1}{A_{Siv} C_{Siv}^h}\, A_{UT,d}^{Siv,h-\bar{h}}(x_B). \tag{15}$$

For the $\cos\phi_h$ asymmetry we have:

$$A_{UU,d}^{\cos\phi_h,h-\bar{h}}(x_B) = \Phi(x_B)\,(\underbrace{C_{Cahn}^h}_{\text{const.}} + 2\mathcal{N}_{BM}^{Q_V}(x_B)\, \underbrace{C_{BM}^h}_{\text{const.}}), \tag{16}$$

$$\Phi(x_B) = \frac{\sqrt{\pi}\,(2-\bar{y})\sqrt{1-\bar{y}}}{\langle Q \rangle\,[1+(1-\bar{y})^2]}, \tag{17}$$

$$\bar{y} = \frac{\langle Q \rangle^2}{2 M_d E\, x_B}, \tag{18}$$

where $\langle Q \rangle^2$ is the value of Q^2 for each x_B-bin.

Using Eqs.(15, 17) we get the following relation between Sivers and $\cos\phi_h$ asymmetries:

$$A_{UU,d}^{\cos\phi_h,h-\bar{h}}(x_B) = C_{\widetilde{BM}}^h\, \Phi(x_B)\, A_{UT,d}^{Siv,h-\bar{h}}(x_B) + C_{Cahn}^h\, \Phi(x_B). \tag{19}$$

Analogously, for the $\cos\phi_h$ asymmetry we have:

$$A_{UU,d}^{\cos 2\phi_h,h-\bar{h}}(x_B) = \hat{\Phi}(x_B)\,(\mathcal{N}_{BM}^{Q_V}(x_B)\, \underbrace{\hat{C}_{BM}^h}_{\text{const.}} + \frac{M M_d}{\langle Q \rangle^2}\, \underbrace{\hat{C}_{Cahn}^h}_{\text{const.}}), \tag{20}$$

where

$$\hat{\Phi}(x_B) = \frac{2\,(1-\bar{y})}{[1+(1-\bar{y})^2]} \tag{21}$$

and M is the proton mass. Therefore,

$$A_{UU,d}^{\cos 2\phi_h,h-\bar{h}}(x_B) = \hat{C}_{\widetilde{BM}}^h\, \hat{\Phi}(x_B)\, A_{UT,d}^{Siv,h-\bar{h}}(x_B) + \frac{M M_d}{\langle Q \rangle^2}\, \hat{\Phi}(x_B)\, \hat{C}_{Cahn}^h \tag{22}$$

We want to make some comments on eqs.(19, 22). As a result of the usage of differential asymmetries in these equations there are no sum over quark flavour, no parton density Q_V (which cancels out, being the same in the numerator and denominator of any asymmetry), no sea quarks distributions, no transverse momentum distributions. The different x_B-dependences of the Cahn and BM contributions, allow us to disentangle them and thus provide two independent ways for extracting the Cahn contribution from data.

3. Tests of eq.(12) using eqs.(19, 22) on the COMPASS data for deuteron target

Using the COMPASS data about Sivers and $\langle \cos\phi_h \rangle$ and $\langle \cos 2\phi_h \rangle$ asymmetries we construct on the basis of eq.(6) the corresponding differential asymmetries which are shown on Fig.(2). Some

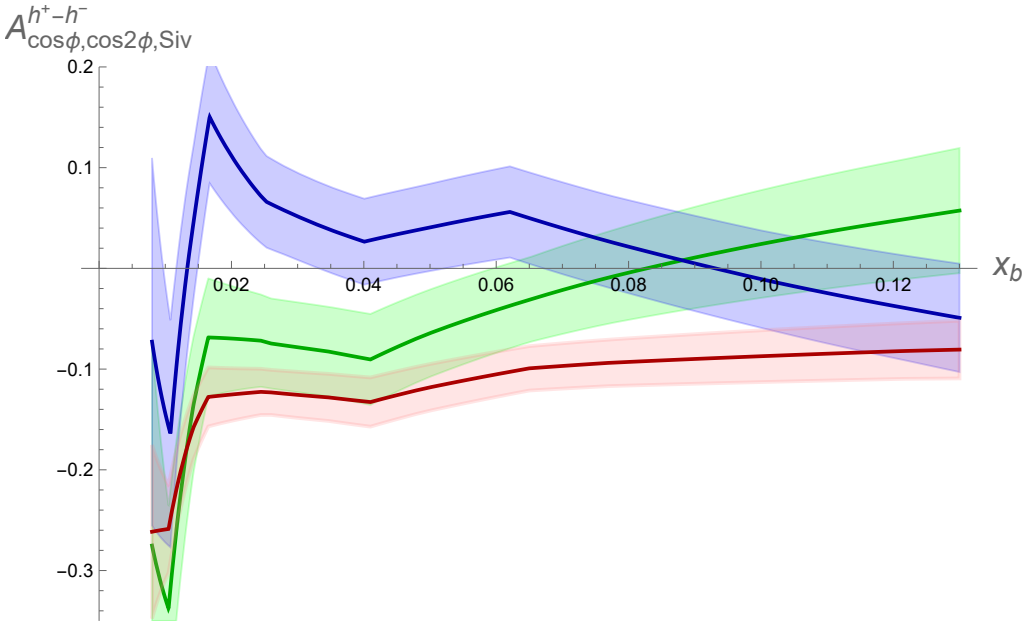

Figure 2: $A^{Siv,h^+-h^-}_{UT,d}(x_B)$ (blue), $A^{\cos\phi_h,h^+-h^-}_{UU,d}(x_B)$ (red) and $A^{\cos 2\phi_h,h^+-h^-}_{UU,d}(x_B)$ (green) with corresponding $\pm 1\sigma$ error bands.

technical remarks are needed at this point. First, it has been mentioned already that we work in the Q^2 interval where the Q^2-dependence of some collinear PDF's and FFs can be neglected. Moreover, because of using differential asymmetries we need collinear distributions of valence quarks only (u_V and d_V in our case). Using the available CTEQ parametrizations for the PDFs [22], we see that there is almost no Q^2-dependence in the valence-quark distributions u_V and d_V in almost the whole Q^2 range covered by COMPASS. More specifically we work in the interval $Q^2 \in [1.77, 16.27]$ GeV^2 which implies $x_B \in [x_i, x_f] = [0.014, 0.13]$. Second, in the calculation of the errors we assume that data are not correlated. Third, the data for different asymmetries are given at different Q^2 bins. Therefore, in order to compare them we need to interpolate the data. The data seems rather chaotic, so we choose linear interpolation and work with the interpolation functions in our analysis. This reflects to the χ^2 we minimize which are:

$$\chi^2_{cos\,\phi} = \frac{1}{x_f - x_i}\int_{x_i}^{x_f} dx\, \frac{\left[F_{exp}(x) - F_{th}(x)\right]^2}{\left[\Delta F_{exp}(x)\right]^2}, \tag{23}$$

$$\chi^2_{cos\,2\phi} = \frac{1}{x_f - x_i}\int_{x_i}^{x_f} dx\, \frac{\left[\hat{F}_{exp}(x) - \hat{F}_{th}(x)\right]^2}{\left[\Delta \hat{F}_{exp}(x)\right]^2}. \tag{24}$$

Here

$$F_{exp}(x_B) = A_{UU,d}^{\cos\phi_h,h^+-h^-}(x_B) - C_{\widetilde{BM}}^h \sqrt{\frac{\pi}{\langle Q^2\rangle}}\, A_{UT,d}^{Siv,h^+-h^-}(x_B), \quad (25)$$

$$F_{th}(x_B) = C_{Cahn}^h \sqrt{\frac{\pi}{\langle Q^2\rangle}}, \quad (26)$$

$$\hat{F}_{exp}(x_B) = A_{UU,d}^{\cos 2\phi_h,h^+-h^-}(x_B) - \hat{C}_{\widetilde{BM}}^h\, \hat{\Phi}(x_B)\, A_{UT,d}^{Siv,h^+-h^-}(x_B), \quad (27)$$

$$\hat{F}_{th}(x_B) = \frac{MM_d}{\langle Q\rangle^2(x_B)}\, \hat{C}_{Cahn}^h\, \hat{\Phi}(x_B). \quad (28)$$

The fitting parameters are C_{Cahn}^h and $C_{\widetilde{BM}}^h$ for eq.(23) and, respectively, $\hat{C}_{Cahn}^h$ and $\hat{C}_{\widetilde{BM}}^h$ for eq.(24). Note that in both cases the "experimental" data F_{exp} and $\hat{F}_{exp}$ contain fitting parameters. As a result the errors $\Delta F_{exp}(x_B)$ and $\Delta\hat{F}_{exp}(x_B)$ contain fitting parameters as well and the fits are non-linear.

The result of the fit of eq.(19) minimizing χ^2 defined in eq.(23) is:

$$C_{\widetilde{BM}}^h = 0.54 \pm 0.80 \quad (29)$$

$$C_{Cahn}^h = -0.165 \pm 0.043 \quad (30)$$

and graphically is depicted on Fig.(3).

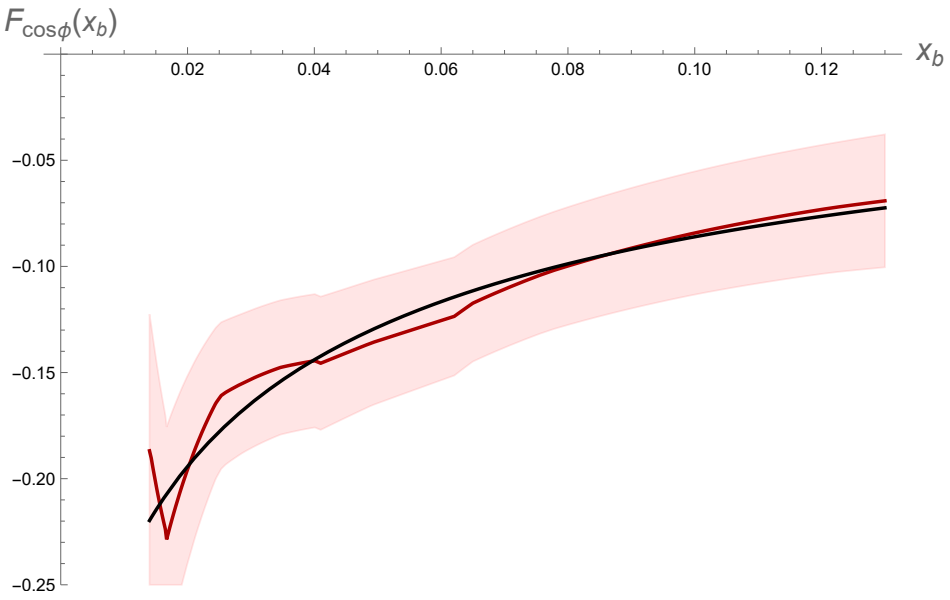

Figure 3: The result of the eq.19 test: The black line is F_{th} (eq.(26)), the red one is F_{exp} (eq.(25)), $\chi^2_{cos\,\phi} = 0.035$. The $\pm 1\sigma$ error band is the light red region.

The result of fitting eq.(22) using the χ^2 defined in eq.(24) is:

$$\hat{C}_{\widetilde{BM}}^h = -1.6 \pm 1.6 \quad (31)$$

$$\hat{C}_{Cahn}^h = 0.045 \pm 0.124 \quad (32)$$

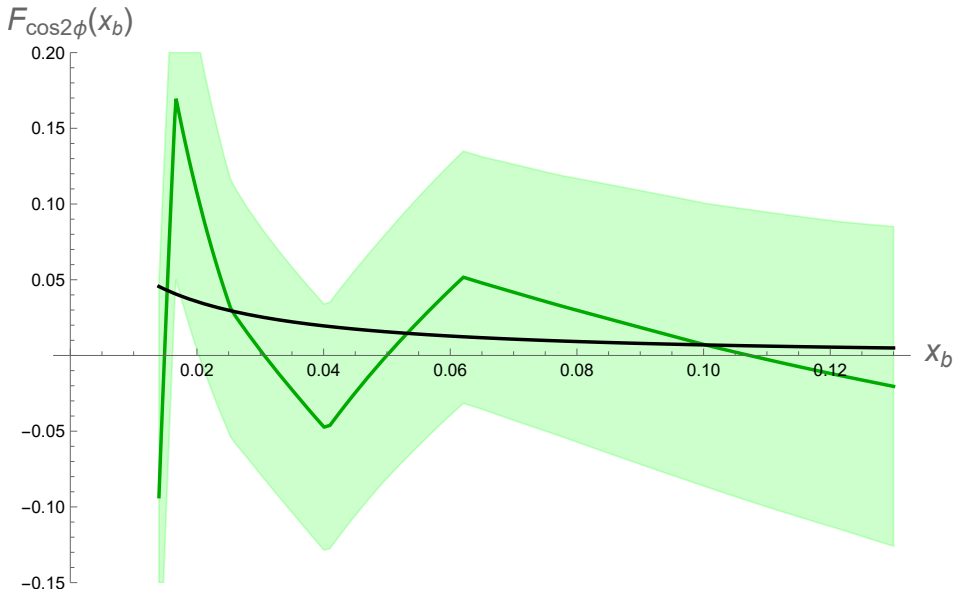

Figure 4: Fitting eq.22: The black line is $\hat{F}_{th}$ (eq.(28)), the green one is $\hat{F}_{exp}$ (eq.(27)), $\chi^2_{cos\,2\phi} = 0.13$. The $\pm 1\sigma$ error band is the light green region.

and graphically is depicted on Fig.(4).

In both cases we have excellent agreement between theory and experiment which supports the truthfulness of our assumption given in eq.(12).

4. Cahn coefficients and the transverse momentum distributions parameters

Both Cahn coefficients we have just determined from our fits can be expressed in a close form using Collins FFs.

$$C^h_{Cahn} = -\langle k^2_\perp \rangle \frac{\int dz_h\, z_h [D^h_{Q_V}(z_h)]/\sqrt{\langle P^2_T \rangle}}{\int dz_h\, [D^h_{Q_V}(z_h)]}, \tag{33}$$

$$\hat{C}^h_{Cahn} = \frac{1}{M M_d \langle k^2_\perp \rangle \langle p^2_\perp \rangle} \frac{\int dz_h [D^h_{Q_V}(z_h)]\, J(z_h)}{\int dz_h\, [D^h_{Q_V}(z_h)]}. \tag{34}$$

Here $J(z_h) = \int dP^2_T\, e^{-\frac{P^2_T}{\langle p^2_\perp \rangle}} \int dk^2_\perp k^2_\perp e^{-k^2_\perp \frac{\langle P^2_T \rangle}{\langle k^2_\perp \rangle \langle p^2_\perp \rangle}} \int_0^{2\pi} d\phi\, \cos 2\phi\, e^{a \cos\phi}$, $a = (2 z_h k_\perp P_T)/\langle p^2_\perp \rangle$, $\langle P^2_T \rangle = \langle p^2_\perp \rangle + z^2_h \langle k^2_\perp \rangle$, $\langle p^2_\perp \rangle$ is the TMD-FFs parameter (the analog of $\langle k^2_\perp \rangle$) and D are Collins functions [15]. For each quark Collins functions are parameterized in [21] and tabulated in http://lapth.cnrs.fr/ffgenerator/ From them and because of the neglected Q^2-dependence we can construct Collins functions for sum of valence quarks

$$D^h_{Q_V}(z_h, Q^2) = e^2_u D^h_{u_V}(z_h, Q^2) + e^2_d D^h_{d_V}(z_h, Q^2), \tag{35}$$

where, analogously to the PDFs u_V and d_V used earlier, $D^h_{q_V}(z_h, Q^2) = D^h_q(z_h, Q^2) - D^h_{\bar{q}}(z_h, Q^2)$.

The problem which is central in present work is the controversy in the literature about the values of $\langle k_\perp^2 \rangle$ and $\langle p_\perp^2 \rangle$ which take part in eqs.(33,34). There are (at least) four incompatible estimates:

1. According to Ref.[14], where an analysis of the old EMC [16] and FNAL [17] SIDIS data has be done
$$\langle k_\perp^2 \rangle = 0.25\,\mathrm{GeV}^2 \quad \text{and} \quad \langle p_\perp^2 \rangle = 0.20\,\mathrm{GeV}^2. \tag{36}$$
2. According to Ref.[18]
$$\langle k_\perp^2 \rangle = 0.18\,\mathrm{GeV}^2 \quad \text{and} \quad \langle p_\perp^2 \rangle = 0.20\,\mathrm{GeV}^2. \tag{37}$$
The result is based on the P_T-spectrum of HERMES data and Monte Carlo calculations.
3. In Ref.[13] there are two sets of values. The first one, extracted from HERMES data [19] is
$$\langle k_\perp^2 \rangle = 0.57 \pm 0.08\,\mathrm{GeV}^2 \quad \text{and} \quad \langle p_\perp^2 \rangle = 0.12 \pm 0.01\,\mathrm{GeV}^2, . \tag{38}$$
4. The second result in Ref. [13] which is extracted from COMPASS data [20] is
$$\langle k_\perp^2 \rangle = 0.61 \pm 0.20\,\mathrm{GeV}^2 \quad \text{and} \quad \langle p_\perp^2 \rangle = 0.19 \pm 0.02\,\mathrm{GeV}^2. \tag{39}$$

Note that eqs.(33, 34) in fact define Cahn coefficients as functions of parameters $\langle p_\perp^2 \rangle$ and $\langle k_\perp^2 \rangle$. Therefore, we can try to solve eqs.(30, 32) with respect to $\langle p_\perp^2 \rangle, \langle k_\perp^2 \rangle$. An excellent fit (in the interval $\langle p_\perp^2 \rangle \in [0.01, 0.5]$) of eq.(30) considered as an implicit function is

$$\langle k_\perp^2 \rangle = 0.0457386 + 0.960348\langle p_\perp^2 \rangle - 1.61132\langle p_\perp^2 \rangle^2 + 1.99264\langle p_\perp^2 \rangle^3. \tag{40}$$

Analogously, an excellent fit (again in the interval $\langle p_\perp^2 \rangle \in [0.01, 0.5]$) of eq.(32) considered as an implicit function is

$$\langle k_\perp^2 \rangle = 0.0290194 + 0.698747\langle p_\perp^2 \rangle - 1.61602\langle p_\perp^2 \rangle^2 + 2.3786.\langle p_\perp^2 \rangle^3 \tag{41}$$

The roots of the difference of right hand sides of eqs.(40,41) determine $\langle p_\perp^2 \rangle$ and from it either from eq.(40) or from eq.(41) — $\langle k_\perp^2 \rangle$. Unfortunately, two of the roots are nonphysical an one is far outside the interval in which the fits are determined. The situation is best illustrated graphically, see Fig.5: The two curves $C^h_{Cahn}(\langle p_\perp^2 \rangle, \langle k_\perp^2 \rangle) = -0.165$ and $\hat{C}^h_{Cahn}(\langle p_\perp^2 \rangle, \langle k_\perp^2 \rangle) = 0.045$ are identical if the errors are taken into account which prevents determination of $\langle p_\perp^2 \rangle$ and , $\langle k_\perp^2 \rangle$. The intersection of their error corridors (which should determine the error of the $\langle p_\perp^2 \rangle$ and , $\langle k_\perp^2 \rangle$) coincides with the error corridor of $C^h_{Cahn}(\langle p_\perp^2 \rangle, \langle k_\perp^2 \rangle) = -0.165$.

5. Conclusions

We have successfully tested twice the assumption that BM and Sivers functions of sum of valence quarks (in the case of deuteron target) are proportional. Note that the corresponding fits are quite unusual: The data we have fitted are combinations of experimental data with fitting parameters

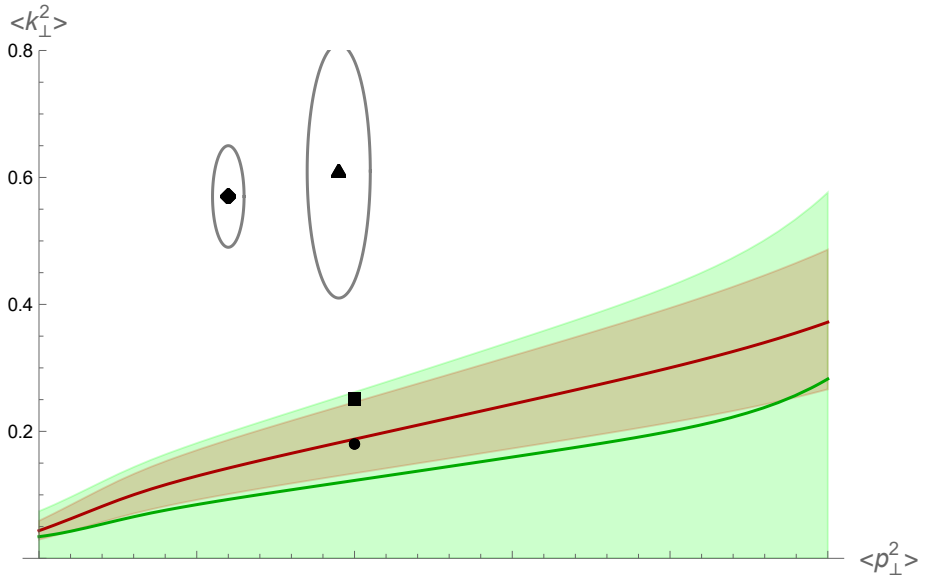

Figure 5: Red line: $C^h_{Cahn}(\langle p_\perp^2\rangle, \langle k_\perp^2\rangle) = -0.165$ with $\pm 1\sigma$ error band in light red. Green line: $\hat{C}^h_{Cahn}(\langle p_\perp^2\rangle, \langle k_\perp^2\rangle) = 0.045$ with $\pm 1\sigma$ error band in light green. The values of $\langle p_\perp^2\rangle$ and $\langle k_\perp^2\rangle$ given in eqs.(36–39) are indicated by black circle, box, diamond and triangle respectively.

participating in them — see eqs.(25,27). As a result, the fitting parameters appear in the data errors as well. This make the fits highly nonlinear and nontrivial.

It is interesting to compare our result to the one obtained in Refs. [11, 12]. The assumption which has been considered in these articles is that BM and Sivers functions are proportional for each quark and anti quark separately. This assumption and the one considered here (eq.(12) would be in agreement if the coefficients of proportionality for the valence quarks and anti quarks, found in Refs. [11, 12], are the same, i.e. $\lambda_u \approx \lambda_{\bar{u}} \approx \lambda_d \approx \lambda_{\bar{d}} \approx \lambda_{Q_V}$. However, this is not the case and the discrepancy is much beyond the error, determined by the experiment. We think that our result is more reliable because it is based entirely on measurable quantities. Therefore, our conclusion is that the values of $\lambda_u, \lambda_{\bar{u}}, \lambda_d$ and $\lambda_{\bar{d}}$ given in Refs. [11, 12] are not correctly determined.

We have determined the kinematical Cahn contributions, both directly from the fits and from calculations. The calculated values are very sensitive to the parameters of the transverse momentum distributions $\langle k_\perp^2\rangle$ and $\langle p_\perp^2\rangle$ in the unpolarized PDFs and FFs, respectively. We use this dependence in an attempt to determine $\langle p_\perp^2\rangle$ and $\langle k_\perp^2\rangle$ from the values of Cahn coefficients, determined while testing BM to Sivers relation. The exact determination fails because of newly revealed correlation between C^h_{Cahn} and $\hat{C}^h_{Cahn}$ functions which is interesting in its own ground. Nevertheless, our result selects eqs.(36, 37) from the list of available values of $\langle p_\perp^2\rangle$, $\langle k_\perp^2\rangle$.

6. Acknowledgement

The work is supported by Grant KP-06-N58/5 of the Bulgarian Science Fund.

References

[1] R. P. Feynman, The Behavior of Hadron Collisions at Extreme Energies. High Energy Collisions: Third International Conference at Stony Brook, (1969), N.Y. Gordon & Breach. pp. 237–249. ISBN 978-0-677-13950-0.

[2] D. Boer and P.J.Mulders, Phys. Rev. **D 57** 5780 (1998)

[3] D.Sivers, Phys. Rev. **D41** (1990) 83; **43** 261 (1991)

[4] A. Bacchetta, F. Conti, and M. Radici, Phys. Rev. D 78 074010 (2008), arXiv:0807.0323.

[5] A. Courtoy, S. Scopetta, and V. Vento, Phys. Rev. D 80, 074032 (2009), arXiv:0909.1404.

[6] B. Pasquini and F. Yuan, Phys. Rev. D 81, 114013 (2010), arXiv:1001.5398.

[7] E. Christova, E. Leader, and M. Stoilov, Phys. Rev. D 97, 056018 (2018), arXiv:1705.10613.

[8] E. Christova, Phys. Rev. **D90** (2014) 054005 (arXiv:1407.5872)

[9] E. Christova and E. Leader, Phys. Rev. **D92** (2015) 114004 (arXiv:1507.01399)

[10] M. Anselmino, et al. Phys. Rev. D **83** (2011) 114019 (arXiv:1101.1011)

[11] V. Barone, A. Prokudin and Bo-Qiang Ma, Phys. Rev. **D 78**, 045022 (2008)

[12] Vincenzo Barone, Stefano Melis and Alexej Prokudin, Phys. Rev. **D 81**, 114026 (2010)

[13] M. Anselmino et al., JHEP **04** (2014)005, arXiv:1312.6261

[14] M. Anselmino et al., Phys. Rev. **D71**, 074006 (2005), arXiv:hep-ph/0501196.

[15] J.C.Collins, Nucl. Phys. **B 396** 161 (1993)

[16] EMC Collaboration, M. Arneodo et al., Z. Phys. **C34** (1987) 277

[17] Fermilab E665 Collaboration, M.R. Adams et al., Phys. Rev. **D48** (1993) 5057

[18] F.Giordano, report No DESY-THESIS-2008-030

[19] A. Airapetian et al. (HERMES Collaboration), Phys. Rev. **D87**, 074029 (2013)

[20] C. Adolph et al. (COMPASS), Eur. Phys. J. **C73**, 2531 (2013).

[21] S. Albino, B. A. Kniehl and G. Kramer, Nucl. Phys. B803 (2008) 42

[22] The Durham HepData Project, http://hepdata.cedar.ac.uk/pdf/pdf3.html